Cathodoluminescence of stacking fault bound excitons for local probing of the exciton diffusion length in single GaN nanowires

Gilles Nogues, Thomas Auzelle, Martien Den Hertog, Bruno Gayral, Bruno Daudin

Cathodoluminescence of stacking fault bound excitons for local probing of the exciton diffusion length in single GaN nanowires

Gilles Nogues,[1, 2, a)] Thomas Auzelle,[3] Martien Den Hertog,[1, 2] Bruno Gayral,[3] and Bruno Daudin[3]

[1)] *Univ. Grenoble Alpes, Inst. NEEL, F-38042 Grenoble, France*
[2)] *CNRS, Inst. NEEL, F-38042 Grenoble, France*
[3)] *CEA, INAC, F-38054 Grenoble, France*

(Dated: 12 March 2014)

We perform correlated studies of individual GaN nanowires in scanning electron microscopy combined to low temperature cathodoluminescence, microphotoluminescence and scanning transmission electron microscopy. We show that some nanowires exhibit well localized regions emitting light at the energy of a stacking fault bound exciton (3.42 eV) and are able to observe the presence of a single stacking fault in these regions. Precise measurements of the cathodoluminescence signal in the vicinity of the stacking fault gives access to the exciton diffusion length near this location.

Carrier diffusion length is a key quantity in optoelectronics, as it notably plays a significant role in the competition between radiative and non-radiative processes, especially in materials with large densities of defects. Concerning nitride semiconductors, various studies have established that carrier diffusion length in InGaN and GaN bidimensional (2D) layers are rather small, in the range of 50-250 nm[1–7]. Such lengths are smaller than the typical distance between dislocations[8], one among other possible reasons for the surprising efficiency of radiative recombination in InGaN quantum wells in spite of the high density of defects in current heterostructures. With the aim of further efficiency improvement, a current trend in nitride optoelectronics research is to explore the potential of nanowires (NWs) as building-blocks for light emission or absorption devices. This approach has already led to the realization of NW heterostructure-based light-emitting diodes (LEDs)[9–12]. In the case of these pioneering works, the small diameter of NWs raises the issue of the influence of size effects on carrier diffusion. More generally, the issue of carrier diffusion length in GaN NWs is poorly documented to date. Recent works[13–15] suggest that recombinations are faster in InGaN nanorods than in 2D layers, which is correlated to a smaller carrier diffusion length and has been tentatively assigned to possible surface damage. In this letter we address the issue of exciton diffusion length in single GaN NWs with a diameter in the range of 100 nm. For this purpose, low-temperature cathodoluminescence (CL) experiments have been performed on individual NWs in correlation with microphotoluminescence (µPL) and scanning transmission electron microscopy (STEM) studies that reveal the presence of I1 basal stacking faults (SFs). It is well known from 2D-layer studies that such SFs are radiative recombination centers[16–18]. Previous TEM/CL studies on GaN epilayers have already evidenced the correlation between the presence of different types of SFs with well identified emission peaks[16,17]. The density of structural defects was relatively large in those samples. In the case of our NWs, we show that emission peaks are linked to the presence of a single defect, acting as a quasi-punctual recombination center. By varying the distance between the SF and the the CL excitation spot we investigate the diffusion length along the NW axis.

The nanowires are grown by Plasma-assisted Molecular Beam Epitaxy (MBE) on a 2-inch Si(111) substrate. Desoxydation of the silicon is done in situ by annealing at 950 °C until the clear appearance of the 7×7 surface reconstruction at 820 °C. The growth temperature, set at 820 °C, is determined by the measurement of the corresponding Ga desorption time[19,20]. A thin AlN buffer layer (2-3 nm thick) is grown directly onto the silicon. Used as a seed layer for the GaN nanowires, it decreases the tilt of the NWs relative to the normal to the surface[21]. This helps to obtain well separated nanowires, even for extensive growth time. NWs were grown for 18 h in N-rich conditions (Ga/N ratio of 0.3)[22]. They are $L =3$ µm long and their diameters range from 50 to 100 nm.
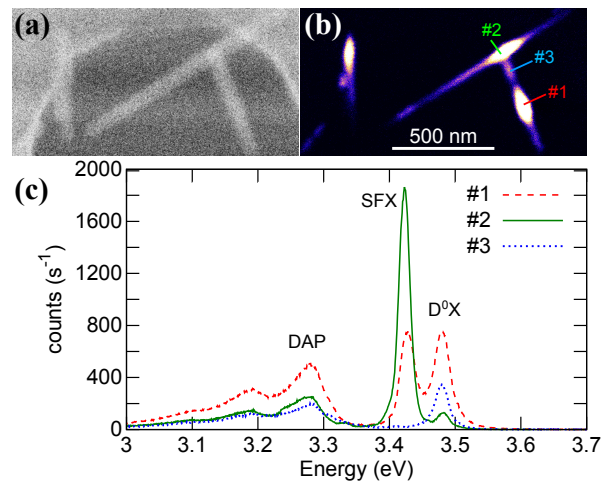

FIG. 1. (a) SEM image of 3 dispersed NWs. (b) Corresponding image of the CL signal between 3.40 eV and 3.50 eV. (c) CL spectra at 5 K with a spot excitation at points #1 to #3 shown on (b).

a)Electronic mail: gilles.nogues@neel.cnrs.fr

As grown NWs are mechanically dispersed onto 2 kinds of substrates. Substrate S1 is used for CL and μPL studies. It is made of a Si wafer. Localization marks are patterned by standard deep UV (DUV) optical lithography followed by reactive ion etching (RIE), using the resist as a mask. It is then sputtered with a 100 nm-thick Al layer and a 20 nm-thick SiO_2 layer. For combined TEM and CL studies, substrate S2 consists of a home-made 35 nm thick Si_3N_4 membrane with a window size of 90 μm. Arrays of nitride membranes are fabricated starting from a 200 μm thick Si (100) wafer with a layer of low stress Si_3N_4 of 35 nm on top of a 240 nm thick SiO_2 layer on each side. The fabrication procedure is described in Ref.[23], with the difference that for these membranes the SiO_2 layer is removed below the Si_3N_4 layer by RIE and a sequential KOH etch. Optical DUV lithography and electron beam metallization are used to pattern Ti-Au markers on the membranes to locate the same NW in different experiments.

CL images are taken at 5 K in a FEI scanning electron microscope (SEM) and analyzed through a 45 cm spectrometer and UV-optimized grating with 600 grooves/mm. Figures 1(a-b) present simultaneously recorded SEM and CL images of 3 NWs on substrate S1. The color scale of the CL image is set in order to show that light comes from the whole length of the NWs. Nevertheless, a strong emission arises from 3 bright spots which saturate the image. Figure 1(c) presents three spectra with a fixed electron beam excitation at three locations (#1 to #3) shown on image 1(b). The spectrum #3 is representative of the emission from the whole length and is similar to the ensemble PL measurements on the as-grown sample. One observes a peak at 3.48 eV that corresponds to the emission from neutral donor bound exciton (D^0X) and a peak at 3.28 eV with its phonon replica at lower energy that are attibuted to donor-acceptor pairs (DAP). Spectra #2 and #3 show that the bright spots are associated to an extra emission peak at 3.42 eV attributed to the emission from excitons trapped by stacking faults (SFX)[16,24,25]. CL observations allow us to locate well isolated NWs with SFX emission that are further studied by microphotoluminescence. μPL spectra are similar to Fig. 1(c) with a magnitude of the 3.42 eV peak slightly smaller or comparable to the D^0X one. This is well understood by considering that the laser excitation spot is larger than the NW and that the μPL spectrum integrates light emitted over its whole volume. The linewidth of the D^0X peak varies significantly from one NW to the other between 2 and 20 meV, whereas the 3.42 eV peak linewidth is always in the 10-20 meV range. The larger linewidth of the 3.42 eV peak has been reported before[26] and is still of unknown origin.

Further evidence of the correlation between the emission at 3.42 eV and the presence of a SF is given by joint CL and STEM studies of the same NW on a S2 substrate. A well isolated NW is first identified in low-temperature CL [Figs. 2(b-d)]. It displays a localized emission at 3.42 eV near one of its tips. The D^0X signal
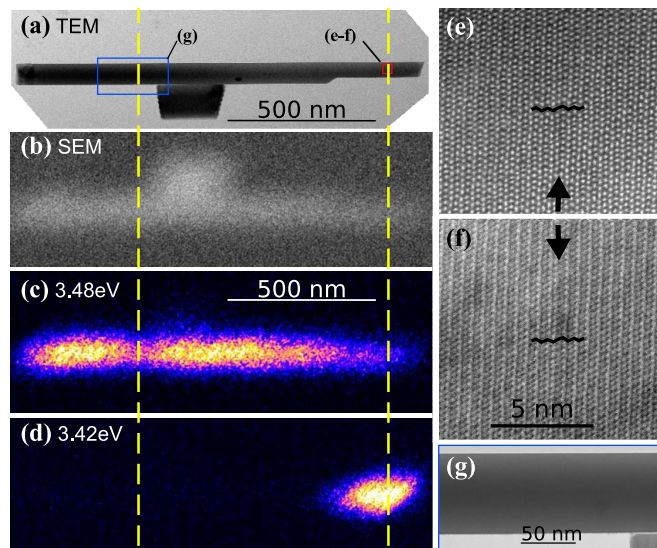

FIG. 2. Same NW observed in BF STEM (a), SEM (b), CL at 3.48 eV (c) and 3.42 eV (d). (e) HAADF STEM and (f) BF STEM images of the region marked by a red rectangle in (a). (g) BF STEM zoom on the blue rectangle in (a).

is more homogeneous, except for two areas where it is quenched. One of them corresponds to the place where the 3.42 eV emission occurs, the other one is in the middle of the NW. In Figure 2(a) a bright field scanning TEM (BF STEM) image of the same NW is shown oriented along the [2-1-10] direction. We note that between the two observations, the NW remained at the same location but rotated onto itself. It explains why the small piece of GaN attached to the NW is at different positions between Figs. 2(a) and (b). The region marked by the red rectangle in Fig. 2(a) is shown at higher magnification in BF STEM [Fig. 2(f)] and high angular dark field (HAADF) STEM images [Fig. 2(e)] which reveal the presence of a stacking fault. For sake of clarity it is indicated by an arrow in both images, as well as a line following the stacking of the Ga columns in the 2H hexagonal wurtzite structure (ABABA.. stacking), that is disrupted by the insertion of one C plane (..ABABCAC.. stacking) characteristic of a cubic zinc blende phase. Comparison of the CL and STEM data clearly shows that the 3.42 eV emission exhibits an excellent spatial correlation with the location of the SF. On the other hand Fig. 2(g) shows a higher magnification BF STEM image of the region indicated with the blue rectangle in Fig 2(a), that is correlated with a quenching of D^0X CL emission. In this region we observe no feature indicating the presence of crystal defects. A continuous smooth contrast over this region was confirmed by high resolution STEM, as for the rest of the NW (not shown here).

The profile of the CL signal along the NW longitudinal axis at 3.42 eV is therefore related to the probability for an exciton to be trapped by a single SF acting as a radiative recombination center. We define $n_{FX}(x,t)$ (resp. n_{D^0X} and n_{SFX}) as the linear density of free excitons
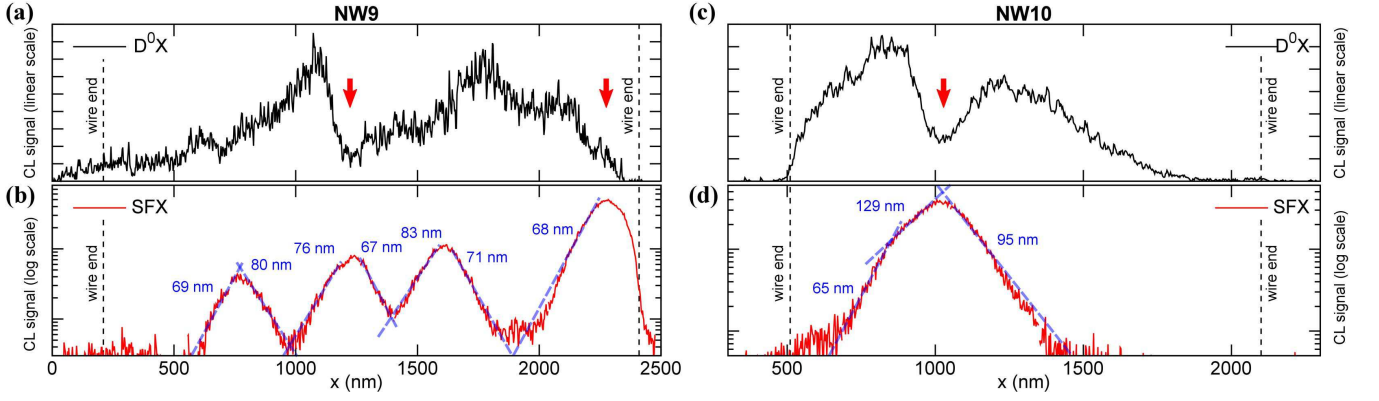
FIG. 3. CL intensity profiles along the longitudinal coordinate x for two nanowires NW9 (a-b) and NW10 (c-d). (a) and (c): D^0X signal in linear scale. Arrows mark localized areas where it is unambiguously quenched by the presence of a SF. (b) and (d): SFX signal in log scale. Dashed lines are exponential fits with characterisctic length L_{NW} indicated next to each line.

(FX) (resp. neutral donor and SF bound excitons) between x and $x + dx$. Extending the model of Corfdir et al.[18], and using the same assumptions (absence of non-radiative decay channels and detrapping processes of bound excitons), one writes:

$$\frac{\partial n_{FX}}{\partial t} = D\frac{\partial^2 n_{FX}}{\partial x^2} + p(x) - \left(\frac{1}{\tau_{r,FX}} + \frac{4s}{d}\right)n_{FX} \quad (1)$$
$$- \left[\frac{1}{\tau_{FX\to D^0X}} + \frac{1}{\tau_{FX\to DAP}} + \gamma_{FX\to SFX}(x)\right]n_{FX},$$

where D is the diffusion constant of the FX in the material. $p(x)$ represents the excitation term. It is assumed constant over the wire length in µPL. On the contrary it is point like in the case of CL. The FX population can decay either radiatively, with time $\tau_{r,FX}$, or through surface effect, s being the surface recombination velocity and d the NW diameter[27]. The last line of Eq. 1 corresponds to the trapping of free excitons by neutral donors (characteristic time $\tau_{FX\to D^0X}$), DAPs ($\tau_{FX\to DAP}$) or the SF. In the latter case, $\gamma_{FX\to SFX}(x)$ has a non zero value $1/\tau^0_{FX\to SFX}$ only close to the SF, with a characteristic extension w_{SF}. In the same manner one has:

$$\frac{\partial n_{D^0X}}{\partial t} = \frac{n_{FX}}{\tau_{FX\to D^0X}} - \frac{n_{D^0X}}{\tau_{r,D^0X}}, \quad (2)$$

$$\frac{\partial n_{SFX}}{\partial t} = \gamma_{FX\to SFX}(x)n_{FX} - \frac{n_{SFX}}{\tau_{r,SFX}}, \quad (3)$$

where τ_{r,D^0X} (resp. $\tau_{r,SFX}$) is the radiative decay time of the neutral donor (resp. stacking fault) bound exciton. The total SFX (resp. D^0X) fluorescence signal is $\int_{-L/2}^{L/2} n_{SFX}/\tau_{r,SFX}dx$ (resp. $\int n_{D^0X}/\tau_{r,D^0X}dx$). µPL observations show that their stationary values have the same amplitude. Hence the SF capture rate is dramatically larger than the one of the neutral donors, in agreement with the results of Ref.[18]. From Eqs. 2 and 3, one infers $\tau^0_{FX\to SFX} \simeq \tau_{FX\to D^0X} * w_{SF}/L$. Using a SF capture

range[24] $w_{SF} = 3$ nm, $1/\tau^0_{FX\to SFX}$ is 300 times larger than the capture rate by neutral donors.

We now assume a single NW extending from $-L/2$ to $L/2$ and containing a single SF at $x = 0$. It is excited at position x_p by the electron beam, $p(x) = p_0\delta(x - x_p)$. Outside the SF capture range, the stationnary solution to Eq. 1 is $n_{FX}(x) = n_0 \exp(-|x - x_p|/L_{NW})$, where $L_{NW} = \sqrt{D\tau_{eff}}$ is the diffusion length in the NW, with:

$$\frac{1}{\tau_{eff}} = \frac{1}{\tau_{r,FX}} + \frac{4s}{d} + \frac{1}{\tau_{FX\to D^0X}} + \frac{1}{\tau_{FX\to DAP}}. \quad (4)$$

Time-resolved photoluminescence experiments in ensemble of GaN nanorods reported $\tau_{r,FX} \simeq 100$ ps[28,29] and $s = 2.7\ 10^4$ cm/s[13,14]. In the set of NWs we have studied $d = 110\pm10$ nm. Hence the two first terms of Eq. 4 contribute with the same magnitude to the effective decay rate of the FX. The capture rate by neutral donors or DAPs depends on their density. For pure undoped thick layers of GaN, CL experiments report exciton diffusion lengths in the vicinity of threading dislocations ranging from $L_{2D} = 81$[30] to 201 nm[31]. In our NW sample, the absence of a peak at the FX energy and the presence of D^0X and DAP peaks in the spectra let us infer that the capture rate $1/\tau_{FX\to D^0X} + 1/\tau_{FX\to DAP}$ is larger than the radiative or surface decay terms.

Close to a SF, the effective decay rate $1/\tau_{eff}$ is dominated by the SF capture rate $1/\tau^0_{FX\to SFX}$, which is L/w_{SF} larger than the D^0X capture rate. The corresponding diffusion length is therefore divided by a factor $\sqrt{L/w_{SF}}$. It is in the 10 nm range, of the same order of magnitude as w_{SF}. This means that a large fraction of incoming excitons is trapped by the SF and later converted into a photon. The SF fluorescence signal is therefore proportional to $n_{FX}(x = 0) = n_0 \exp(-|x_p|/L_{NW})$.

Figures 3(b) and (d) plot the CL signal in logscale as a function of the longitudinal wire coordinate x for two different NWs on a S1 substrate. The peaks are well fitted by convoluting an exponential decay with a Gaussian function of width $w_p = 30\pm10$ nm for electron acceleration

voltages $V \geq 10$ kV. This is larger than w_{SF} and rather reflects the size of the excitation region by the electron beam. For $V = 5$ kV, w_p is degraded to 70 nm. We attribute this effect to backscattered electrons in the NW at lower energy. At distances larger than w_p from the peak center, the tails on each side are well fitted by exponential functions with characteristic length L_{NW} (dashed lines). Average of L_{NW} measured for an ensemble of 12 NWs gives $L_{\mathrm{NW}} = 68 \pm 16$ nm $< L_{2D}$. Based on the previous discussion, it confirms that the capture by of neutral donors or DAP dominates the FX effective decay rate. We also observe a large dispersion on the values of L_{NW}, with sometimes abrupt changes like around $x = 800$ nm on Fig. 3(d). This is evidence of long range variations of $1/\tau_{\mathrm{eff}}$. The latter can arise from changes of the density of neutral donors or DAPs or the presence of an extra non radiative decay term $-n_{\mathrm{FX}}/\tau_{\mathrm{nr,FX}}(x)$ in Eq. 1 due to other kind of impurities.

Further evidence of long range variations of the NW parameters is given by the CL signal at the $D^0 X$ emission energy [Figures 3(a) and (c)]. Its amplitude variations can only be accounted for if one assumes that $\tau_{\mathrm{FX} \rightarrow D^0 X}$ varies along the wire length or if one adds an extra non radiative decay term $-n_{D^0 X}/\tau_{\mathrm{nr},D^0 X}(x)$ to Eq. 2 due to the trapping of the $D^0 X$ by other defects. For example, a SF can capture excitons from the neighboring neutral donors[18] resulting in a localized quenching area [arrows on Figs. 3(a,c)]. However, we also observe extended NW areas where a partial quenching of the signal occurs. This can only happen if the previously introduced capture or decay rates experience long range variations and are not just point-like as for the SF defects. We observe no clear correlation between the $D^0 X$ signal magnitude and L_{NW}. This means that $1/\tau_{\mathrm{eff}}$ is determined by other parameters like DAP capture rate or non radiative decay.

In conclusion, we are able to observe single SFs present in individual NWs with different optical and structural techniques. The CL profile in the vicinity of a SF is well understood by a simple diffusion model of the exciton.

[1] J. Speck and S. Rosner, Physica B **273 - 274**, 24 (1999).

[2] S. J. Rosner, E. C. Carr, M. J. Ludowise, G. Girolami, and H. I. Erikson, Appl. Phys. Lett. **70**, 420 (1997).

[3] S. J. Rosner, G. Girolami, H. Marchand, P. T. Fini, J. P. Ibbetson, L. Zhao, S. Keller, U. K. Mishra, S. P. DenBaars, and J. S. Speck, Appl. Phys. Lett. **74**, 2035 (1999).

[4] T. Sugahara, H. Sato, M. Hao, Y. Naoi, S. Kurai, S. Tottori, K. Yamashita, K. Nishino, L. T. Romano, and S. Sakai, Jpn. J. Appl. Phys. **37**, L398 (1998).

[5] S. Sonderegger, E. Feltin, M. Merano, A. Crottini, J. F. Carlin, R. Sachot, B. Deveaud, N. Grandjean, and J. D. Ganière, Appl. Phys. Lett. **89**, 232109 (2006).

[6] V. Liuolia, S. Marcinkevičius, Y.-D. Lin, H. Ohta, S. P. DenBaars, and S. Nakamura, J. Appl. Phys. **108**, 023101 (2010).

[7] S. Chichibu, K. Wada, and S. Nakamura, Appl. Phys. Lett. **71**, 2346 (1997).

[8] M. Godlewski, E. Łusakowska, E. Goldys, M. Phillips, T. Böttcher, S. Figge, D. Hommel, P. Prystawko, M. Leszczynski, I. Grzegory, and S. Porowski, Appl. Surf. Sci. **223**, 294 (2004).

[9] A. Kikuchi, M. Kawai, M. Tada, and K. Kishino, Jpn. J. Appl. Phys. **43**, L1524 (2004).

[10] G. Tourbot, C. Bougerol, A. Grenier, M. Den Hertog, D. Sam-Giao, D. Cooper, P. Gilet, B. Gayral, and B. Daudin, Nanotechnology **22**, 075601 (2011).

[11] A.-L. Bavencove, G. Tourbot, J. Garcia, Y. Désières, P. Gilet, F. Levy, B. André, B. Gayral, B. Daudin, and L. S. Dang, Nanotechnology **22**, 345705 (2011).

[12] W. Guo, A. Banerjee, P. Bhattacharya, and B. S. Ooi, Appl. Phys. Lett. **98**, 193102 (2011).

[13] J. B. Schlager, K. A. Bertness, P. T. Blanchard, L. H. Robins, A. Roshko, and N. A. Sanford, J. Appl. Phys. **103**, 124309 (2008).

[14] Y. Park, M. Holmes, Y. Shon, I. Yoon, H. Im, and R. Taylor, Nanoscale Research Letters **6**, 81 (2011).

[15] H.-S. Chen, Y.-F. Yao, C.-H. Liao, C.-G. Tu, C.-Y. Su, W.-M. Chang, Y.-W. Kiang, and C. C. Yang, Optics Letters **38**, 3370 (2013).

[16] G. Salviati, M. Albrecht, C. Zanotti-Fregonara, N. Armani, M. Mayer, Y. Shreter, M. Guzzi, Y. V. Melnik, K. Vassilevski, V. A. Dmitriev, and H. P. Strunk, Phys. Status Solidi A **171**, 325 (1999).

[17] R. Liu, A. Bell, F. A. Ponce, C. Q. Chen, J. W. Yang, and M. A. Khan, Appl. Phys. Lett. **86**, 021908 (2005).

[18] P. Corfdir, P. Lefebvre, J. Levrat, A. Dussaigne, J.-D. Ganière, D. Martin, J. Ristić, T. Zhu, N. Grandjean, and B. Deveaud-Plédran, J. Appl. Phys. **105**, 043102 (2009).

[19] O. Landré, R. Songmuang, J. Renard, E. Bellet-Amalric, H. Renevier, and B. Daudin, Appl. Phys. Lett. **93**, 183109 (2008).

[20] R. Mata, K. Hestroffer, J. Budagosky, A. Cros, C. Bougerol, H. Renevier, and B. Daudin, J. Cryst. Growth **334**, 177 (2011).

[21] R. Songmuang, O. Landré, and B. Daudin, Appl. Phys. Lett. **91**, 251902 (2007).

[22] M. Sanchez-Garcia, E. Calleja, E. Monroy, F. Sanchez, F. Calle, E. Muñoz, and R. Beresford, J. Cryst. Growth **183**, 23 (1998).

[23] M. I. den Hertog, F. González-Posada, R. Songmuang, J. L. Rouviere, T. Fournier, B. Fernandez, and E. Monroy, Nano Letters **12**, 5691 (2012).

[24] Y. T. Rebane, Y. G. Shreter, and M. Albrecht, Phys. Status Solidi A **164**, 141 (1997).

[25] C. Stampfl and C. G. Van de Walle, Phys. Rev. B **57**, R15052 (1998).

[26] O. Brandt, C. Pfüller, C. Chèze, L. Geelhaar, and H. Riechert, Phys. Rev. B **81** (2010).

[27] W. Shockley, *Electrons and Holes in Semiconductors* (Van Nostrand, Princeton, NJ, 1950).

[28] C. I. Harris, B. Monemar, H. Amano, and I. Akasaki, Appl. Phys. Lett. **67**, 840 (1995).

[29] L. Lahourcade, J. Renard, B. Gayral, E. Monroy, M. P. Chauvat, and P. Ruterana, J. Appl. Phys. **103**, 093514 (2008).

[30] N. Pauc, M. R. Phillips, V. Aimez, and D. Drouin, Appl. Phys. Lett. **89**, 161905 (2006).

[31] N. Ino and N. Yamamoto, Appl. Phys. Lett. **93**, 232103 (2008).